Int J Theor Phys (2009) 48: 1271–1289
DOI 10.1007/s10773-008-9899-3

Stability of Circular Orbits in General Relativity: a Phase Space Analysis

A. Palit · A. Panchenko · N.G. Migranov · A. Bhadra · K.K. Nandi

Published online: 18 November 2008

Abstract Phase space method provides a novel way for deducing qualitative features of nonlinear differential equations without actually solving them. The method is applied here for analyzing stability of circular orbits of test particles in various physically interesting environments. The approach is shown to work in a revealing way in Schwarzschild spacetime. All relevant conclusions about circular orbits in the Schwarzschild-de Sitter spacetime are shown to be remarkably encoded in a *single* parameter. The analysis in the rotating Kerr black hole readily exposes information as to how stability depends on the ratio of source rotation to particle angular momentum. As a wider application, it is exemplified how the analysis reveals useful information when applied to motion in a refractive medium, for instance, that of optical black holes.

Keywords Gravitational field · Circular orbits · Stability · Dynamical systems

A. Palit (✉) · K.K. Nandi
Department of Mathematics, University of North Bengal, Siliguri 734 013, India
e-mail: mail2apalit@gmail.com

K.K. Nandi
e-mail: kamalnandi1952@yahoo.co.in

A. Bhadra
High Energy and Cosmic Ray Research Center, University of North Bengal, Siliguri 734 013, India
e-mail: aru_bhadra@yahoo.com

A. Panchenko · N.G. Migranov · K.K. Nandi
Joint Research Laboratory, Bashkir State Pedagogical University, Ufa 450000, Russia

A. Panchenko
e-mail: alex.souljaa@gmail.com

N.G. Migranov
e-mail: ufangm@yahoo.co.uk

1 Introduction

It is well known that in Einstein's theory of General Relativity (GR) motion in a gravitational field is described by a system of dynamical equations. The nonlinear ordinary differential equation for the path is obtained by eliminating the affine parameter from that system of equations. An important class of solutions of the path equation is formed by circular trajectories. The issue of their stability is particularly important in confinement problems and/or in accretion phenomenon in astrophysics. However, conventional analysis of stability of orbits essentially deals with *dynamical* equations involving the affine parameter and a potential function. On the other hand, potential functions may not always be immediately evident, for instance, in a simulated environment like moving refractive dielectrics whereas path equations in them could follow directly from Fermat's principle or Hamilton-Jacobi equation. Therefore, a natural query is to ask if information about stability of circular orbits can be obtained from the *geometrical* path equation alone. Our aim here is to rigorously demonstrate that it is indeed possible via phase space analysis of autonomous systems corresponding to various physically interesting environments. To our knowledge, such a useful application in gravitational physics seems yet unavailable in the literature.

For our analysis, we shall not require any other information beyond the path equation. The conserved angular momentum appearing in it will allow us to connect the phase space results with actual kinematics. An equilibrium state corresponds to a constant solution of a differential equation describing a mechanical system and conversely. Constant solution means that velocity $\dot{x}$ and acceleration $\ddot{x}$ be simultaneously zero. The concept of stability of an equilibrium state is borrowed from the familiar example of motion of a pendulum about the equilibrium point $x = 0$ and $\dot{x} = 0$ where x is angle with the vertical. The motion is stable because a small displacement from the equilibrium position will lead to only small oscillations of the bob about that position in a vertical plane. Different closed paths on the phase space about a stable equilibrium point correspond to real oscillations with different periods. If the paths around an equilibrium point is such that a small displacement from the equilibrium state takes the system far away from that point, it is called an unstable equilibrium point. For instance, the equilibrium point $x = \pi$ and $\dot{x} = 0$ is an unstable saddle in the pendulum motion. There is no closed path around such equilibrium point although some paths may pass through it depending on the values of the parameter. Open paths not passing through an equilibrium point represent whirling motion of the pendulum [1].

In this paper, we shall portray path equations for different solutions of GR as plane autonomous dynamical systems and study them through phase space and/or Hamiltonian analysis. Of particular interest is the treatment in cosmological scenario and in the Kerr metric. As a further example, the method is applied to light propagation in a medium relevant to optical black holes and interesting information obtained.

The article is intended for theoretical physicists in general and practicing relativists in particular. The contents are organized as follows. In Section 2, we briefly describe the path equation needed for our purpose. Section 3 treats the path equation as an autonomous system without the cosmological constant $\lambda = 0$. Section 4 treats the autonomous system as a Hamiltonian system. Section 5 deals with the case $\lambda \neq 0$. In Sect. 6, we discuss circular motion in Kerr spacetime. Section 7 shows an example applying the method to light motion in a refractive medium relevant to optical black holes. Section 8 summarizes the obtained results. We take $G = c_0 = 1$, unless specifically restored.

2 Path Equation

A spherically symmetric static solution of the Einstein field equations for a mass M is given by the Schwarzschild-de Sitter solution (SdS) in standard coordinates $(x^\alpha) \equiv (t, r, \theta, \phi)$:

$$\begin{aligned} d\tau^2 &= B(r)dt^2 - B^{-1}(r)dr^2 - r^2 d\theta^2 - r^2 \sin^2\theta d\phi^2, \\ B(r) &= 1 - \frac{2M}{r} - \frac{\lambda r^2}{3} \end{aligned} \tag{1}$$

where $\lambda > 0$ is the cosmological constant. The cosmological constant $\lambda \sim 10^{-55}$ cm^{-2} > 0 is responsible for dark energy that explains the currently observed accelerated cosmic expansion [2–4]. The case $\lambda < 0$ (anti-de Sitter) is observationally ruled out and we shall not deal with this case here. The case $M \neq 0$, $\lambda = 0$ corresponds to the pure Schwarzschild solution and $r_H = 2M$ is the horizon radius so that the metric is valid for $r > r_H$. When $M = 0$, $\lambda \neq 0$ we have pure de Sitter solution which can be reexpressed in such a manner that it represents an expanding space devoid of matter.

When $M \neq 0$, $\lambda \neq 0$, there occur two horizons provided that $0 < \lambda < \lambda_{crit} = \frac{1}{9M^2}$. The black hole horizon appears at $r_h = \frac{1}{\sqrt{\lambda M^2}} \cos\frac{\pi+\xi}{3}$ and the cosmological horizon at $r_c = \frac{1}{\sqrt{\lambda M^2}} \cos\frac{\pi-\xi}{3}$ where $\xi = \cos^{-1}(\sqrt{3}\lambda M^2)$. The spacetime is dynamic for $r < r_h$ and for $r > r_c$. At the critical value $\lambda = \lambda_{crit}$, the two horizons coincide at $r_{ph} = 3M$. The static radius r_{st} is defined as a hypersurface where the attraction due to M balances the cosmic repulsion due to λ and is given by [5]

$$r_{st} = \left(\frac{3M}{\lambda}\right)^{\frac{1}{3}}. \tag{2}$$

All circular orbits are bounded from below by $r = r_{ph}$ and from above by the static radius $r = r_{st}$.

Following conventional stability analyses of circular orbits involving a potential function $V(r)$, we obtain the expression

$$\left.\frac{d^2V}{dr^2}\right|_{r=R} = -\left(\frac{2M}{R^3}\right)\left(\frac{\frac{4}{3}\lambda R^4 - 5\lambda M R^3 + R - 6M}{R - 3M}\right). \tag{3}$$

In the case $\lambda = 0$, it follows from (3) that stable circular orbits may exist only at radii $R > 6M$. At $R = 6M$, $\frac{d^2V}{dr^2}\,|_{r=R} = 0$ which indicates that it is a point of inflection. When $R \to +\infty$ and $3M+$, we have $\frac{d^2V}{dr^2} \to 0-$ and $+\infty$ respectively. The first limit indicates stability in the asymptotic region while the divergent second limit indicates instability.

Defining $u = \frac{1}{r}$, we have the path equation on the equatorial plane $\theta = \pi/2$ for a particle as

$$\ddot{x} = a + bx + cx^2 + dx^{-3} \tag{4}$$

where an overdot denotes differentiation with respect to ϕ and

$$x = u = \frac{1}{r}, \tag{5}$$

$$a = \frac{M}{h^2}, \tag{6}$$

$$b = -1, \tag{7}$$

$$c = 3M, \tag{8}$$

$$d = -\frac{\lambda}{3h^2}, \tag{9}$$

$$h = r^2 \frac{d\phi}{d\tau} = \text{const.} \tag{10}$$

The quantity h is the conserved angular momentum. Equation (4) with the defined coefficients is all we need.

We shall study it in the phase plane ($x = u$, $y \equiv \frac{du}{d\phi}$) posing it as an autonomous system as follows

$$\dot{x} = y, \tag{11}$$

$$\dot{y} = a + bx + cx^2 + dx^{-3}. \tag{12}$$

Equilibrium points of the system are given by

$$\dot{x} = 0, \qquad \dot{y} = 0. \tag{13}$$

The first equation gives circular orbits $r = R = \text{const.}$ and the second equation gives the angular momentum h along that orbit

$$h^2 = \frac{MR(1 - \frac{\lambda}{3M}R^3)}{1 - \frac{3M}{R}}. \tag{14}$$

It follows that $h^2 = 0$ at $R = r_{st}$ and $h^2 = \infty$ at $R = 3M$. Let us now consider the case $\lambda = 0$ corresponding to the Schwarzschild spacetime.

3 Case I: $\lambda = 0$

The autonomous system

$$\dot{x} = y, \tag{15}$$

$$\dot{y} = a + bx + cx^2 \tag{16}$$

gives two equilibrium points (x, y) at

$$P: \quad \left(\frac{-b + \sqrt{b^2 - 4ac}}{2c}, 0\right); \qquad Q: \quad \left(\frac{-b - \sqrt{b^2 - 4ac}}{2c}, 0\right).$$

In order to have these points located on the real phase plane, we have to assume $b^2 - 4ac \geq 0$ or rephrasing, $\alpha^2 \equiv 1 - \frac{12M^2}{h^2} \geq 0$. We have introduced the shorthand α for notational convenience. Each choice of α gives a corresponding equilibrium point or a value of the radius r. Let us first consider the degenerate case $\alpha = 0$ and study the stability of corresponding radius.

Case (a): $k^2 \equiv b^2 - 4ac = 0 \Rightarrow a = \frac{b^2}{4c} \neq 0$.

The equilibrium point on the phase plane occurs only at $(-\frac{b}{2c}, 0)$. Eliminating the parameter a, the autonomous system (15), (16) can be reduced to the following set of equations

$$\dot{x} = y, \tag{17}$$

$$\dot{y} = \frac{1}{4c}(b + 2cx)^2. \tag{18}$$

The differential phase path is given by

$$\frac{dy}{dx} = \frac{(b + 2cx)^2}{4cy} \tag{19}$$

which integrates to

$$y^2 = \frac{1}{12c^2}(b + 2cx)^3 + A \tag{20}$$

where A is an arbitrary constant of integration.

We see that the parameter b has the effect of only translation in the variable x while c introduces magnification in both x and y. Thus the GR correction term c can be regarded as the dominating parameter among a, b and c. By the translation

$$y' = y, \tag{21}$$

$$x' = x + \frac{b}{2c} \tag{22}$$

the autonomous system (15), (16) further reduces to

$$\dot{x}' = y', \tag{23}$$

$$\dot{y}' = cx'^2 \tag{24}$$

which gives a one-parameter family of phase paths

$$3y'^2 = 2cx'^3 + C \tag{25}$$

on the phase plane (x', y') where C is an arbitrary parameter. The phase paths for $M = 1$ (or $c = 3$) and different values of C are given in Fig. 1.

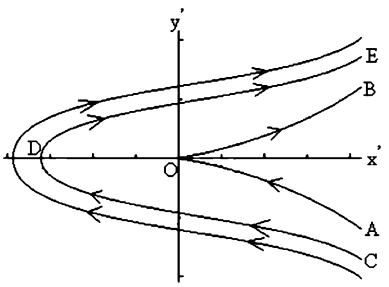

Fig. 1 The origin O is a cusp (see p. 19, Ref. [1]). Path AO leads to the origin while OB leads away from O. These paths correspond to $C = 0$. For $C \neq 0$, the paths CDE never reach O and the motion is analogous to the whirling motion of the bob of a pendulum

The equilibrium point has now been shifted to the origin $(0, 0)$ which gives

$$x' = 0 \Rightarrow r = 6M \Rightarrow hu \equiv r\frac{d\phi}{d\tau} = \text{const}, \tag{26}$$

$$y' = 0 \Rightarrow -h\frac{du}{d\phi} \equiv \frac{dr}{d\tau} = 0. \tag{27}$$

From the above, we immediately learn the following: The equilibrium point corresponds, in the physical (r, ϕ) plane, to a circular orbit of radius $6M$ with the test particle having a constant cross radial velocity hu and a zero radial velocity $-h\frac{du}{d\phi}$. From the overall pattern of the phase paths given in Fig. 1, we see that a small displacement from the equilibrium state can take the system on a phase path which leads it far away from the equilibrium state. The dynamical condition for this to happen is given by

$$\alpha^2 = 0 \Rightarrow h^2 = 12M^2. \tag{28}$$

Although the phase path (25) is independent of a, it applies only to massive test particles because the value of h^2 becomes infinity for light ($d\tau = 0$). In this case, the condition (28) becomes obviously inapplicable. We shall treat this case separately in Sect. 4.

Let us analyze in a little more detail the paths in different quadrants in Fig. 1. A typical initial state (x_0', y_0') on the phase plane is as follows

$$x_0' = x_0 + \frac{b}{2c} = x_0 - \frac{1}{6M} = \delta, \tag{29}$$

$$y_{0\pm}' = y_{0\pm} = \pm\sqrt{\frac{6x_0'^3 + C}{3}} = \pm\sqrt{\frac{6\delta^3 + C}{3}} \tag{30}$$

where $C > -6\delta^3$. These equations will allow us to closely examine phase paths in the neighborhood of the equilibrium point. We see from (29) that the GR allowed open interval $x_0^{-1} = r_0 \in (2M, +\infty)$ is mapped onto a finite open interval $x_0' \in (-\frac{1}{6M}, \frac{1}{3M})$ around the equilibrium point $(0, 0)$. This interval can be subdivided into two parts for δ or x_0'.

One part is $\delta \in [0, \frac{1}{3M})$ corresponding to $6M \geq r_0 > 2M$. This interval refers to points (x_0', y_{0+}') on the paths in first quadrant and to points (x_0', y_{0-}') on the paths in the fourth quadrant. To proceed further, let us translate (29), (30) to the physical (r, ϕ) plane choosing $C = 0$:

$$r_0 = \frac{6M}{6M\delta + 1}, \tag{31}$$

$$\left.\frac{du}{d\phi}\right|_{0\pm} = \pm\sqrt{2\delta^3} \Rightarrow \left.\frac{dr}{d\tau}\right|_{0\pm} \equiv -h\left(\frac{du}{d\phi}\right)_{0\pm} = \mp h\sqrt{2\delta^3}. \tag{32}$$

(Note that the cross radial component of velocity can be expressed as $r\frac{d\phi}{d\tau} = hx'$ and the radial component as $\frac{dr}{d\tau} = -hy'$.) We find the following distinct possibilities for paths (25) passing through the equilibrium point $(0, 0)$: (i) As δ increases from 0 to $\frac{1}{3M}$, we see from (29), (30) that both x_0' and y_{0+}' increase from the equilibrium point $(0, 0)$ which implies that the phase point in the first quadrant moves outward (to the right), as represented by OB in Fig. 1. Correspondingly, from (32), we see that u increases with ϕ which indicates that the radius r_0 undergoes a decrease in time τ from $6M$ to $2M$ (as reflected in $\frac{dr}{d\tau}\,|_+ = -h\sqrt{2\delta^3} <$

0). (ii) As δ decreases from $\frac{1}{3M}$ to 0, we see that both x_0' and y_{0-}' decrease to the equilibrium point $(0,0)$ which implies that the phase point in the fourth quadrant moves inward (to the left), as represented by AO in Fig. 1. Correspondingly, u decreases with ϕ and the radius r_0 undergoes an increase in time τ from $2M$ to $6M$ (as reflected in $\frac{dr}{d\tau}\mid_{-} = +h\sqrt{2\delta^3} > 0$). For $C \neq 0$, paths will not pass through $(0,0)$ but parts of CDE lying in the first and fourth quadrant can be interpreted similarly.

The other part is $\delta \in (-\frac{1}{6M}, 0]$, for which $\infty > r_0 \geq 6M$. This represents points only on the second and third quadrant (where $x_0' = \delta < 0$). In this case, to avoid imaginary quantity in (32), we must choose $C \neq 0$, that is, we have to deal with the full set of (29), (30). For different values of $C \neq 0$ in Fig. 1, we see that the phase paths like CDE are not closed around the equilibrium point. (These paths are analogous to whirling motion of pendulum.) It is clear that most of the paths in the interval $-\frac{1}{6M} \leq x_0' < \frac{1}{3M}$, when slightly displaced from the equilibrium point $(0,0)$, neither converge to it nor form a center about it. In fact, the phase paths resemble exactly those around a *cusp* [1]. This leads us to conclude that the equilibrium point $(0,0)$ corresponding to radius $r = 6M$ is neither stable or nor unstable because of the dynamically degenerate condition $\alpha = 0$. This conclusion will be further supported in Sect. 4.

Case (b): $k^2 \equiv b^2 - 4ac > 0$

There are now two distinct equilibrium points occurring at $(\frac{-b+k}{2c}, 0)$ and $(\frac{-b-k}{2c}, 0)$. They combine into a single representative point $(\frac{-b+\alpha}{2c}, 0)$ where $\alpha = +k$ or $-k$. Under the translation

$$y' = y, \tag{33}$$

$$x' = x - \frac{\alpha - b}{2c} \tag{34}$$

the autonomous system (15), (16) reduces, after a little algebra, to

$$\dot{x}' = y', \tag{35}$$

$$\dot{y}' = \alpha x' + c x'^2. \tag{36}$$

The equilibrium points in the new (x', y') phase plane are P_1: $(0,0)$ and Q_1: $(-\frac{\alpha}{c}, 0)$. The linearized system of equations near P_1: $(0,0)$ is

$$\dot{x}' = y', \tag{37}$$

$$\dot{y}' = \alpha x'. \tag{38}$$

Comparing it with the general linear system given by

$$\dot{x}' = a_1 x' + b_1 y', \tag{39}$$

$$\dot{y}' = c_1 x' + d_1 y' \tag{40}$$

we find

$$\begin{aligned} &a_1 = 0, \qquad b_1 = 1, \qquad c_1 = \alpha, \qquad d_1 = 0, \\ &p = a_1 + d_1 = 0, \qquad q = a_1 d_1 - b_1 c_1 = -\alpha \end{aligned} \tag{41}$$

so that the discriminant is

$$\Delta \equiv p^2 - 4q = 4\alpha. \tag{42}$$

Hence the equilibrium point $(0, 0)$ will be a center (stable equilibrium) if $\alpha < 0$ and a saddle point (unstable equilibrium) if $\alpha > 0$. Such an abrupt change in the behavior of the system occurs through $\alpha = 0$. Therefore, $\alpha = 0$ can be called a *bifurcation* point.

The above conclusions are supported by the phase paths following from (35) and (36), namely,

$$y'^2 = \alpha x'^2 + \frac{2c}{3}x'^3 + D \tag{43}$$

where D is an arbitrary constant of integration. In the close vicinity of $(0, 0)$ such that $x' \sim 0$ and x'^3 can be neglected, we get

$$y'^2 - \alpha x'^2 = D \tag{44}$$

which represents a family of concentric ellipses for $\alpha = -k < 0$ (Fig. 2, center, stable) and a family of hyperbolas with asymptotes $y' = \pm\sqrt{\alpha}x'$ for $\alpha = +k > 0$ (Fig. 3, saddle point, unstable). Note that $\alpha \sim 1$, since, for physically realistic particle orbits, $\frac{M^2}{h^2} \ll 1$. Thus, as a sample, we have taken $\alpha = \pm k = \pm 0.9$, and $c = 3$ (which means we are taking units in which $M = 1$) and different values of the parameter D in Figs. 2, 3.

Let us see what conclusions we can draw in the physical (r, ϕ) plane. The point $(x', y') \equiv (0, 0)$ shows that the equilibrium radii r depend on the value of h, and hence of α.

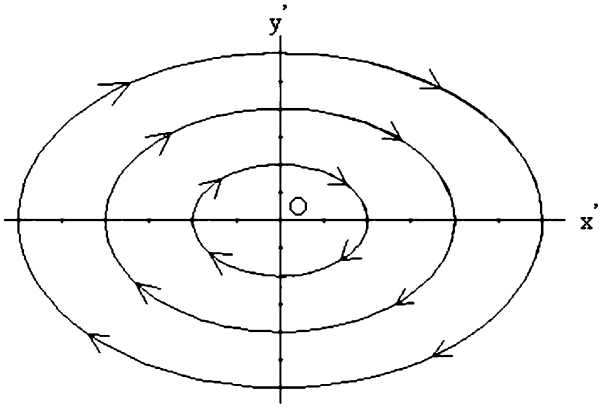

Fig. 2 The origin O is a stable center. Initial conditions slightly shifted from the center take the phase paths on closed elliptic orbits around O. The corresponding motion in physical space is periodic analogous to small oscillations of the bob about downward vertical

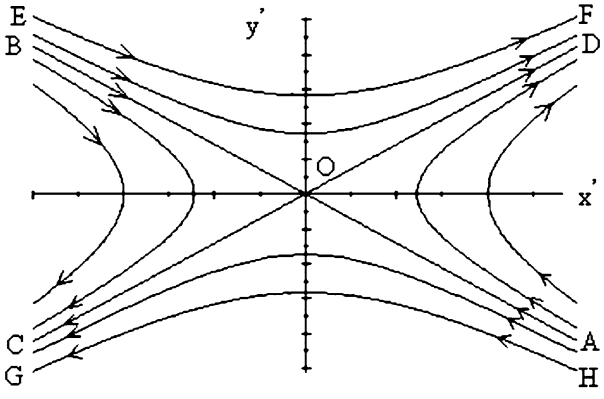

Fig. 3 The origin O is a saddle point. Only the paths AO and BO approach the origin while OC and OD move away from it. Other paths do not lead to the origin. EF, GH represent whirling motion

These radii follow from (34)

$$x' = x - \frac{\alpha - b}{2c} = 0 \Rightarrow r = \frac{6M}{1+\alpha}. \tag{45}$$

This means $\infty > r > 6M$ if $-1 < \alpha < 0$ and $6M > r > 2M$ if $0 < \alpha < 2$. Thus, from what we have learnt from (44), we find that circular orbits with $r > 6M$ are stable (α has negative sign) while those with $r < 6M$ are unstable (α has positive sign). Equation (33) gives

$$y' = y = 0 \Rightarrow \frac{du}{d\phi} = 0 \Rightarrow \frac{dr}{d\tau} = -h\frac{du}{d\phi} = 0 \tag{46}$$

while $r\frac{d\phi}{d\tau} \equiv hu > 0$. That is, the radius r is independent of time while the cross radial velocity $r\frac{d\phi}{d\tau}$ is nonzero. These are exactly what are to be expected of circular motions.

The other equilibrium point $(x', y') \equiv (-\frac{\alpha}{c}, 0)$ corresponds to

$$-\frac{\alpha}{c} = x - \frac{\alpha - b}{2c} \Rightarrow r = \frac{6M}{1-\alpha}. \tag{47}$$

In the close vicinity of this equilibrium point, we may define

$$x'' = x' + \frac{\alpha}{c}. \tag{48}$$

When $x'' \sim 0$, neglecting x''^2, we have from (35), (36), the linearized system

$$\dot{x}'' = y'', \tag{49}$$

$$\dot{y}'' = -\alpha x''. \tag{50}$$

Arguing in the same manner as with (37) and (38), we see that we have here a *reverse* situation, viz., the point Q_1: $(-\frac{\alpha}{c}, 0)$ is a saddle for $\alpha = -k < 0$ and a center for $\alpha = +k > 0$. We shall show below that this is indeed the case. For this, we shall investigate stability by posing the autonomous system as a geometrical Hamiltonian system. The latter technique is said to be more reliable than the linearization technique [1].

4 Hamiltonian System

Dropping primes in the autonomous system, (35), (36), the Hamiltonian system can be defined as

$$\frac{\partial H}{\partial x} = -Y(x, y) = -(\alpha x + cx^2), \tag{51}$$

$$\frac{\partial H}{\partial y} = X(x, y) = y. \tag{52}$$

The necessary and sufficient condition for the system (51), (52) to be a Hamiltonian system, namely, $\frac{\partial X}{\partial x} + \frac{\partial Y}{\partial y} = 0$, is fulfilled for all x and y. [Such fulfillment is a special feature of the GR path (4).] Moreover, $\frac{dH}{d\phi} = 0$ and therefore $H(x, y) = \text{const}$ independent of ϕ. From

(51) and (52), we get

$$H(x,y) = -\frac{\alpha}{2}x^2 - \frac{c}{3}x^3 + u(y), \tag{53}$$

$$H(x,y) = \frac{1}{2}y^2 + v(x) \tag{54}$$

where $u(y)$ and $v(x)$ are arbitrary functions subject to the consistency of (53) and (54). These two equations will match only if

$$u(y) = \frac{1}{2}y^2 - C, \tag{55}$$

$$v(x) = -\frac{\alpha}{2}x^2 - \frac{c}{3}x^3 - E \tag{56}$$

where E is an arbitrary constant. The Hamiltonian paths are given by

$$H(x,y) = -\frac{\alpha}{2}x^2 - \frac{c}{3}x^3 + \frac{1}{2}y^2 - E \tag{57}$$

where E is a parameter. It follows that

$$\frac{\partial^2 H}{\partial x^2} = -(\alpha + 2cx), \tag{58}$$

$$\frac{\partial^2 H}{\partial y^2} = 1, \tag{59}$$

$$\frac{\partial^2 H}{\partial x \partial y} = 0. \tag{60}$$

As before, the equilibrium points occur when $X = 0$ and $Y = 0$ which give the points P_1: $(0,0)$ and Q_1: $(-\frac{\alpha}{c}, 0)$. Thus the quantity

$$q_0 \equiv \frac{\partial^2 H}{\partial x^2}\frac{\partial^2 H}{\partial y^2} - \left(\frac{\partial^2 H}{\partial x \partial y}\right)^2 \tag{61}$$

has the following values

$$q_0|_{P_1} = -\alpha, \tag{62}$$

$$q_0|_{Q_1} = \alpha. \tag{63}$$

When $-1 < \alpha < 0$, the equilibrium point P_1 is a stable center since $q_0 > 0$, but Q_1 is an unstable saddle point. For $\alpha > 0$, the conclusions are reversed. These confirm the results of Sect. 3. The value $\alpha = 0$ is a bifurcation point as it represents a transition of the system from a stable center to an unstable saddle and conversely.

We shall now see what result do we get applying the present method to light trajectories for which $a = 0$. From the original set of (15), (16), we see that they lead to the same Hamiltonian set of (51), (52) with the difference that α is now to be replaced by b. The equilibrium points then are P_2: $(0,0)$ and Q_2: $(-\frac{b}{c}, 0)$. The point P_2 implies

$$x = 0 \Rightarrow r \to \infty \tag{64}$$

and the value of $q_0 \mid_{P_2} = -b = 1 > 0$. This implies that P_2 is a center. From this, we learn that light trajectories (straight lines) in asymptotically flat space ($r \to \infty$) are stable. This is an expected result. The other equilibrium point Q_2 implies

$$x = -\frac{b}{c} \Rightarrow r = 3M \tag{65}$$

at which $q_0 \mid_{Q_2} = b = -1 < 0$ showing that Q_2 represents a saddle point. In other words, light orbit at $r = 3M$ is unstable. This shows that the instability of circular orbits of light at $R = 3M$ depends only on the sign of b and is *independent* of the sign of α, unlike in the case of material orbits.

5 Case II: $\lambda \neq 0$

We have to consider the full autonomous system (11), (12) and as usual, the equilibrium points are given by $\dot{x} = 0,\ \dot{y} = 0$. The latter gives the equation

$$g(x) \equiv cx^5 + bx^4 + ax^3 + d = 0, x \neq 0. \tag{66}$$

Since x has to be non-negative, we have to look only for positive roots of $g(x) = 0$. Once the known signs of coefficients are plugged into $g(x) = 0$, we may apply Descartes' rule of signs to see that $g(x) = 0$ can have either one or three positive real roots, the rest are either negative or imaginary. The auxiliary equation $g'(x) = \frac{dg}{dx} = 0$ has two zero roots and two nonzero roots μ_1, μ_2 given by

$$\mu_1 = \frac{-2b - \sqrt{4b^2 - 15ac}}{5c}, \qquad \mu_2 = \frac{-2b + \sqrt{4b^2 - 15ac}}{5c}. \tag{67}$$

The reality of the roots of $g'(x) = 0$ demands that $\gamma^{\,2} \equiv 4b^2 - 15ac \geq 0$. Since $b = -1$ and $c > 0$, we see that $\mu_1 \leq \mu_2$. Let us denote a representative positive root of $g(x)$ by $\eta \neq 0$, that is, $g(\eta) = 0$. The representative equilibrium point is then $(x, y) = (\eta, 0)$. Then we employ the usual operations on (11) and (12), viz., a translation $x' = x - \eta$, $y' = y$, followed by linearization in the neighborhood of $(x', y') = (0, 0)$. The final result is

$$\dot{x}' = y', \tag{68}$$

$$\dot{y}' = \left(\frac{5c\eta^2 + 4b\eta + 3a}{\eta}\right)x'. \tag{69}$$

Using (39)–(42), we get

$$q = -\left(\frac{5c\eta^2 + 4b\eta + 3a}{\eta}\right), \qquad p = 0, \qquad \Delta = 4\left(\frac{5c\eta^2 + 4b\eta + 3a}{\eta}\right). \tag{70}$$

For a meaningful analysis, we must have $q \neq 0$ which means $g'(\eta) \neq 0$, that is, η can not be a repeated root of $g(x) = 0$. Thus, we find that $(x', y') = (0, 0)$ will be a saddle if $q < 0$ and $\Delta > 0$. This is possible if either $\eta < \mu_1$ or $\eta > \mu_2$. The point $(x', y') = (0, 0)$ will be a center if $q > 0$ and $\Delta < 0$ which means $\mu_1 < \eta < \mu_2$. The linearization scheme is not applicable for $\eta = 0$. The important point to note here is that μ_1, μ_2 do not depend on the cosmological constant λ. Thus the constraint $\gamma^2 = 4 - \frac{45M^2}{h^2} \geq 0$ applies to orbits resulting from the effect of M alone. Orbits close to the static radius are not sensitive to this constraint.

With the above general picture in mind, let us numerically study the behavior of approximate roots of $g(x) = 0$ for some choices of h. For a given M the equilibrium points, hence the radii, vary depending on the values of h, or $x_{eq} = x_{eq}(h, \lambda)$. Choosing units in which $M = 1$, and with the values of coefficients given by $c = 3, b = -1, a = h^{-2}, d = -\frac{\lambda}{3h^2}$ the equation $g(x) = 0$ can be rewritten as

$$h^2(3x^5 - x^4) + x^3 - \frac{\lambda}{3} = 0; \quad h \neq 0. \tag{71}$$

We observe the following behavior. When $h^2 \to 0$, we get only one very small root that approximates to the static radius $x_{eq} = x_{st} = (\frac{\lambda}{3})^{\frac{1}{3}} \sim 10^{-18}$. Other roots are imaginary. As we increase h^2 up to $\frac{45}{4}$, we see that the picture remains almost the same, that is, we continue to obtain a single radius of the order of x_{st}. When $h^2 > \frac{45}{4}$ or $\gamma^2 > 0$, we find that there occur three positive roots, one is of the order of the same static radius, but the other two roots correspond to orbits in the vicinity of M. These results confirm that the radii of orbits close to or at the static radius are indeed insensitive to values of γ. Let us consider a specific value $h = 8$ (say), then we have the following equilibrium points: P_1: $(x = x_{st}, y = 0)$, P_2: $(x = 0.016, y = 0)$ and P_3: $(x = 0.316, y = 0)$ while $\mu_1 = 0.012$, $\mu_2 = 0.254$. According to the general discussion above, we expect that P_2 should be a stable center as $\mu_1 < x < \mu_2$ while P_1 and P_3 should be unstable saddles.

Let us confirm the results by the method of Hamiltonian system. Following the same procedure as in Sect. 4, we deduce that

$$H(x, y) = \frac{1}{2}y^2 - \left(ax + \frac{b}{2}x^2 + \frac{c}{3}x^3 - \frac{d}{2}x^{-2}\right) - F \tag{72}$$

where F is an arbitrary parameter. The expression for q_0 is

$$q_0 = -(b + 2cx - 3dx^{-4}) \tag{73}$$

$$= 1 - 6x - \frac{\lambda}{h^2}x^{-4}. \tag{74}$$

From this, we can conclude the following: At the lower bound, that is, at the local photon radius $x_{ph} = 1/3$, we find $q_0 = -1$ since $h^2 = \infty$. Therefore this particular orbit is unstable and the instability is independent of λ. On the other hand, at the static radius, $q_0\,|_{x=x_{st}} > 0$, implying that the photon orbit (again $h^2 = \infty$) is stable at $x = x_{st}$. The stability of light orbits at the static hypersurface is similar to that in the asymptotically flat region discussed in Sect. 4. At $x = \frac{1}{6}$, $q_0 < 0$, hence $R = 6$ is also an unstable radius. Furthermore, $q_0|_{P_2} > 0$ and $q_0|_{P_3} < 0$ confirming earlier expectations. At the static radius $x = x_{st}$, we have $h^2 = 0$, and $\lambda x_{st}^{-4} \sim 10^{16}$ so that $q_0|_{P_1} = -\infty$. This shows that circular material orbit at the static radius (P_1) is unstable.

What then is the upper bound R_{ub} for stable circular material orbits? This can be found by requiring that $q_0 > 0$ or

$$6x + \frac{\lambda}{h^2}x^{-4} < 1. \tag{75}$$

Putting the expression for h^2 from (14), and assuming that $R_{ub} \gg 6$, we find that

$$R_{ub} = 4^{-\frac{1}{3}}\left(\frac{\lambda}{3}\right)^{-\frac{1}{3}} \tag{76}$$

which is slightly smaller than r_{st}. The radii at which orbits begin to be stable can be obtained from $q_0 = 0$ which gives

$$\lambda = h^2 x^4 (1 - 6x), \quad x \neq 0. \tag{77}$$

The maximum of λ is located at $x = \frac{2}{15}$. Again using the expression for h^2 from (14), we get

$$\lambda_{\max} = \frac{4}{5625} \simeq 0.000711. \tag{78}$$

For $\lambda \sim 10^{-55}$ cm^{-2}, the maximum Schwarzschild mass is $M_{\max} = (\frac{\lambda_{\max}}{\lambda})^{\frac{1}{2}} \sim 5.75 \times 10^{20} M_{\odot}$. Stable material circular orbits can exist only at $R > \frac{15}{2}$ corresponding to $\gamma > 0$. This is confirmed by the stability at P_2 ($R \simeq 10$) and instability at P_3 ($R \simeq 3.3$). The values $\lambda_{\max}$ and $R = \frac{15}{2}$ correspond to another critical value $h^2 = \frac{45}{4}$, as may be obtained from (14). We have obtained it here from a totally different consideration, namely, of roots of $g(x) = 0$. For $h^2 \geq \frac{45}{4}$, there exist local stable equilibrium orbits x_{eq} while no stable local x_{eq} exist for $h^2 < \frac{45}{4}$. We see that the restriction $h^2 \geq \frac{45}{4}$ is *weaker* than the previous $h^2 \geq 12$ for the case $\lambda = 0$.

It is remarkable that a *single* parameter q_0 completely reproduces all the results obtained by Stuchlík and Hledík [5], including their numerical value, viz. $y_{c(ms)} = \frac{\lambda_{\max}}{3} = 0.000237$.

The phase space method can also be applied in the pure de Sitter space which corresponds to $\lambda > 0$, $M = 0$. There is now no balance of forces at any radius, hence there is no static radius. The metric with $M = 0$ immediately fixes $a = c = 0$ in $g(x) = 0$. The equilibrium points then occur at $x^4 = -\frac{\lambda}{3h^2}$. This implies that there are no real equilibrium points and we conclude that circular orbits are not possible in this space.

6 Path Equation in Kerr Spacetime

The phase space method can be profitably utilized in the study of motions in a refractive medium as well. For instance, Evans and Rosenquist [6] showed that the equation of optics in a refractive medium of index $n(\vec{r})$ can be effectively rephrased as a Newtonian "$\vec{f} = m\vec{a}$" form of mechanics. This optical-mechanical analogy led via Fermat's principle to a path equation for light in the form

$$\frac{d^2\vec{r}}{dA^2} = \vec{\nabla}\left(\frac{n^2}{2}\right) \tag{79}$$

where A is a stepping parameter defined in Ref. [6] by $dA = n^{-2}dt$. Optical analogues of mechanical quantities are marked by "..". The equation of motion (79) has been subsequently extended in Ref. [7] to include also the motion of material particles. Note that the form of $n(\vec{r})$ can be arbitrarily preassigned depending on the nature of the medium. The relevant quantities in this formalism are the optical version of mechanical quantities. For instance, instead of the classical angular momentum h, its optical analogue "h_0", viz., $h_0 = r^2 \frac{d\phi}{dA}$ is conserved if $n = n(r)$. A specific form of $n = n(r)$ depicting a Schwarzschild gravitational "medium" exactly yielded the path (4) for $\lambda = 0$ [8]. (See also Ref. [9] for another interesting derivation). It is clear that complicated forms of $n(r)$ corresponding to arbitrary spherical media would lead to path equations more complicated than (4). In these cases, the present method might be preferable to conventional methods.

An example is Kerr spacetime which represents a unique rotating black hole solution for $\lambda = 0$. Alsing [10] has extended the "medium" analogy to Kerr spacetime with rotation

parameter J (= angular momentum per unit mass M of the rotating source) and obtained, to first order in $\frac{M}{r}$, the following path equations on the equatorial slice:

$$\frac{d^2u}{d\phi^2}+u-3Mu^2=\frac{M}{L^2}\left[\left(1-\frac{v_0^2}{c_0^2}\right)\left(1-8Mu\frac{J}{L}\right)-2\frac{J}{L}\left(\frac{v_0^2}{c_0^2}\right)\right](\text{part.}) \tag{80}$$

$$=\frac{-2MJ}{L^3}(\text{light}). \tag{81}$$

Here v_0 is the initial velocity of the particle at infinity and L is its conserved total "angular momentum" per unit test mass given by

$$L=\rho^2\frac{d\phi}{dA}-\frac{2MJ}{\rho} \tag{82}$$

where $\rho=re^{-Mr}$. (In the asymptotic region, $n=1$, $A=t$ $\rho=r$ so that, for $J=0$, we have $L=h$, the familiar mechanical angular momentum.) For a particle starting a radial fall from infinity, $L=0$. In this case, with $n(r)\sim 1+\frac{2M}{\rho}$, one obtains to lowest order in $\frac{M}{r}$ that $\frac{d\phi}{dt}=\frac{2MJ}{r^3}$. This implies that the particle starting with an initial radial fall begins to co-rotate with the black hole in its vicinity (Lense-Thirring effect). In general, we shall take $L\neq 0$. Conventionally, the sign of J is taken as positive or negative according as the source rotation is in the counterclockwise or clockwise sense.

To examine stability, we first note that the autonomous system is of the same type as in (15), (16), only the coefficients are different. The next step is to follow the same procedure as in Sect. 3. Applying it for a particle starting at $v_0=0$, we get the equilibrium points in the (x', y') plane at Q_1: $(0,0)$ and Q_2: $(-\frac{\beta}{c},0)$ where

$$\beta=\pm\sqrt{\left(1+\frac{8JM^2}{L^3}\right)^2-\frac{12M^2}{L^2}} \tag{83}$$

which reduces to α when $J=0$. The interesting result is that the reality of β immediately imposes two restrictions, viz., that $J\neq-\frac{L^3}{8M^2}$ and that the quantity under the radical sign in (83) must be positive which implies $(J-J_+)(J-J_-)>0\Rightarrow$ either $J<J_\pm$ or $J>J_\pm$. These restrictions must be respected if circular orbits are to exist at all in Kerr spacetime. Once this is fulfilled, exactly the same arguments about the stability as in Sect. 3 go through under the replacement of α by β.

Case (a): $\beta^2=0$.

This degenerate condition corresponds to two critical values J_+, J_- of J which are

$$J_\pm=\mp\frac{L^3}{8M^2}\left[2\sqrt{3}\frac{M}{L}\pm 1\right]. \tag{84}$$

The phase paths are the same as those given by (25) indicating unstable equilibrium at radii given by

$$r_{\beta=0}^{Kerr}=\frac{6M}{1+\frac{8JM^2}{L^3}}. \tag{85}$$

Putting the values of $J_\pm$ from (84), we find the radii $r_{\beta=0}^{Kerr}=\mp\sqrt{3}L$, which implies that the rotation J of the source has no role in determining the radii of circular orbits if $\beta^2=0$.

Case (b): $\beta^2 > 0$.

The phase paths are the same as (36) with the replacement of α by β. Hamiltonian analysis reveals that Q_1 is a center and Q_2 is a saddle if $\beta < 0$. These conclusions are reversed if $\beta > 0$. Stable circular orbits occur at

$$r^{Kerr}_{\beta\neq 0} = \frac{6M}{(1+\frac{8JM^2}{L^3}) - \sqrt{(1+\frac{8JM^2}{L^3})^2 - \frac{12M^2}{L^2}}}. \tag{86}$$

From the above, it follows that, as $J \to \pm\infty$, the stable radii $r^{Kerr}_{\beta\neq 0}$ go far beyond $6M$. This implies that the rotation J of the source can not bring about stable circular orbits at radii below $6M$ for material test particles. The situation is the same as in the nonrotating case.

Case (c): $a \neq 0$.

For light ($v_0 = c_0$), $a = \frac{-2MJ}{L^3} \neq 0$, hence the equilibrium points occur at R_1: $(0, 0)$ and R_2: $(-\frac{\sigma}{c}, 0)$ where

$$\sigma = \pm\sqrt{1 + \frac{24JM^2}{L^3}}. \tag{87}$$

Arguments similar to *Case (a),* Sect. 3 go through, with the replacement of α by σ. Thus stable radii occur at

$$r^{Kerr}_{Light} = \frac{6M}{1 - \sqrt{1 + \frac{24JM^2}{L^3}}} \tag{88}$$

depending on the sign of σ. When $J = 0$, the orbit has infinite radius. When $-1 \leq \frac{24M^2J}{L^3} < 0$, stable circular orbits will exist for $r^{Kerr}_{Light} \geq 6M$ but when $\frac{24M^2J}{L^3} > 0$, there can not be any stable radius for light because r^{Kerr}_{Light} becomes negative.

7 Optical Black Holes

The advantage of the phase space method is that it can be applied to situations beyond known gravitation theory when a potential function is not always evident. This can occur, for instance, when one deals with a path equation in the environment of a simulated black hole described by a refractive medium with index $n(r)$. Possibility of laboratory creation of such optical black holes exist in view of a remarkable experiment [11] performed in Bose-Einstein condensates. The experiment demonstrated that optical pulses can travel in the condensate with extremely small group velocities, as low as 17 m/s. The group velocity of light in the vicinity of a real gravitational black hole can indeed be arbitrarily low [12]. It has been shown that light motion around a dielectric vortex structure mimics motion around a black hole [13, 14]. Creation of an event horizon would require that the vortex flow be supplemented with a radial flow as well [15]. Interesting physical effects, like optical Aharonov-Bohm effect far away from the vortex core and bending of light near the core, stem from the consideration of a dielectric medium having a velocity field $\vec{u}$ and a varying index of refraction n.

One might obtain the trajectory of light directly from Fermat's principle

$$\delta \int n(\vec{r})dl = 0. \tag{89}$$

The resulting path equation is given by (79) which, on the equatorial plane $\theta = \pi/2$, gives

$$\frac{dr}{d\phi} = \pm \frac{[r^4 n^2(r) - r_i^2 r^2]^{\frac{1}{2}}}{r_i} \tag{90}$$

where r_i is a constant of integration, interpreted as impact parameter. Stability of circular orbits can be easily studied directly once a form for $n(r)$ is given.

A plausible form for $n(r)$ simulating a static dielectric medium of optical black holes has been studied by Marklund, Anderson, Cattani, Lisak and Lundgren [16]. It is given by

$$n^2(r) = 1 + \frac{r_0^2}{r^2} \tag{91}$$

which has a divergence at $r = 0$, and r_0 is a constant. For $r \gg r_0$, $n(r) \sim 1$ and for $r \ll r_0$, $n(r) \sim \frac{r_0}{r}$. Defining, as before, $u = x = \frac{1}{r}$, the autonomous system corresponding to the problem can be written as

$$\dot{x} = y, \tag{92}$$

$$\dot{y} = \varepsilon x, \quad \varepsilon = \frac{r_0^2 - r_i^2}{r_i^2}. \tag{93}$$

The equilibrium point $(0, 0)$ refers to circular orbit only at the asymptotic region $r = \infty$. Taking the limit $r_i \to \infty$, we find $\varepsilon = -1$. Hence the path equation $y^2 - \varepsilon x^2 = C$ represents a family of concentric ellipses around the origin showing that the orbit is stable independent of any finite value of the extent r_0 of inhomogeneity. But *no* circular orbit at a finite radius is possible. This result is quite consistent with the nature of various trajectories analyzed in Ref. [16]. However, a pathological solution of $\dot{y} = 0$ may be imagined by taking $\varepsilon = 0 \Rightarrow r_0^2 = r_i^2$. We find that there is no equilibrium point at all in this case as $\dot{x} \neq 0$ although $\dot{y} = 0$. The latter yields a phase path equation $y = \frac{dx}{d\phi} = \sqrt{C}$ which integrates to give real space trajectory $x \propto \phi$. This is just in the form of Archimedes' spiral $r_i/r = \phi$ as shown in Ref. [16].

We show now that circular orbits are possible in a nonuniformly *moving* medium with a slowly varying refractive index. Under these conditions, Leonhardt and Piwnicki [13, 14] considered a vortex core with a velocity profile decaying away from the core

$$\vec{u} = \frac{W}{r} e_{\widehat{\phi}} \tag{94}$$

where $2\pi W$ is the vorticity. Let us formally introduce the index given by (91) into the Hamilton-Jacobi equation for light motion derived in [13, 14]. The resulting path equation can be translated to the following autonomous system in the far field limit

$$\dot{x} = y, \tag{95}$$

$$\dot{y} = -x + \frac{1}{l_{AB}^2} \left(r_0^2 x + 2 r_0^2 W^2 x^3 + 3 r_0^4 W^2 x^5 \right) \tag{96}$$

where l_{AB} is the Aharonov-Bohm modified angular momentum given by

$$l_{AB} = l + (n^2 - 1) W = l + \frac{r_0^2}{r^2} W. \tag{97}$$

Interestingly, we find that there is only one equilibrium point (apart from the trivial one at $x = r^{-1} = 0$ or $r = \infty$) at a finite radius photon orbit

$$R = \sqrt{3}r_0\left[-1 + \left\{1 + \frac{3(l_{AB}^2 - r_0^2)}{W^2}\right\}^{\frac{1}{2}}\right]^{-\frac{1}{2}}. \tag{98}$$

In order that this radius be real, we must have

$$1 + \frac{3(l_{AB}^2 - r_0^2)}{W^2} \equiv N^2 > 1 \tag{99}$$

where N is real. The quantity q_0 in this case works out to

$$q_0 = -\left(\frac{4}{3}\right)\frac{W^2}{l_{AB}^2}N(1 - N) > 0 \tag{100}$$

if $N > 1$. Thus the orbit is stable. Of course, the conclusion crucially depends on the form of $n(r)$.

We finally mention an interesting similarity between L of (82) and l_{AB} of (97). A light ray approaching radially ($l = 0$) will acquire an angular momentum $(n^2 - 1)W$ near the vortex core very similar to the Lense-Thirring effect. With $n^2 \sim 1 + \frac{4m}{r}$, where m is some constant, we have $\frac{d\phi}{dt} \sim \frac{4mW}{r^3}$. This allows us to identify $2W$ as the angular momentum of the vortex motion.

8 Summary

Phase space analysis has been successfully applied to practically all walks of life, from physics, engineering, biology to social sciences. Somehow its use in gravitational physics seems rather scarce. Our motivation here was to fill that gap. There is certainly room for further development like exploring how other sophisticated techniques from the phase space repertoire could be applied to stability of noncircular orbits or even classical fields.

We obtained information on stability of circular orbits arguing from the geometrical path equation alone. The usefulness of the method is demonstrated in several situations of physical interest. When the cosmological constant $\lambda = 0$, the dimensionless parameter α played a key role in determining the stability of actual orbits in the physical (r, ϕ) space. It was shown that $\alpha = 0$ is a cusp describing a marginal state, viz., the radius $R = 6M$ is neither stable nor unstable. The light orbit at $R = 3M$ is unstable independent of the sign of α and in the asymptotic region it is always stable. All the conclusions were confirmed by the method of Hamiltonian system.

When $\lambda \neq 0$, there occurred either one or three equilibrium points. The one corresponding to static radius does not depend on the parameter γ but depends on λ. We found that, for $\lambda > 0$, trajectories of circular material orbit at the static radius are unstable. However, for light orbits, $h \to \infty$, so that $q_0 = 1$, hence circular light orbits at static radius are *always* stable. These two results help us understand better the nature of the static hypersurface: Even though forces balance at the hypersurface, it is not exactly like the usual flat asymptotic region where both matter and light orbits are stable. The other two equilibrium points are local and already analyzed in Sect. 4. They do not depend on λ implying that circular orbits in the vicinity of M are not influenced by λ. This is a physically consistent result. It was shown

how a single parameter q_0 nicely reproduced all the relevant results about circular orbits in the Schwarzschild-de Sitter spacetime.

We dealt with circular motion of light and massive particles in the equatorial plane of the Kerr black hole. The derived results are new. The restrictions $J < J_{\pm}$ or $J > J_{\pm}$ for the existence of circular orbits were derived. A general parameter β was found that reduces to α under zero rotation, $J = 0$. For the value $\beta^2 = 0$, the rotation J of the source has no role in determining the radii of circular orbits. For $\beta^2 > 0$, we found that even high values of source rotation can not bring about a stable radius below $6M$. These results could be of importance to accretion phenomenon in astrophysics.

Finally, we applied the method to real optical dielectric (static and moving) and obtained consistent results. Here we only discussed a simple example relevant to optical black holes but *any* given form of refractive index $n(r)$ can be similarly handled. The important advantage is that we did not require information on dynamical potential functions, but relied solely on the path equations coming from Fermat's principle or Hamilton-Jacobi equation. Several such path equations corresponding to various refractive media have been worked out in Ref. [6]. It will naturally be of interest to apply the method in the refractive wormhole "media" constructed from exotic matter [17, 18] or in Brans-Dicke theory [19, 20]. Work is underway.

Acknowledgements The authors wish to thank Denis V. Kondratiev and Guzel N. Kutdusova for technical assistance. K.K.N. acknowledges warm hospitality at J.R.L. where part of the work is carried out.

References

1. Jordan, D.W., Smith, P.: Nonlinear Ordinary Differential Equations, 3rd edn. Oxford University Press, Oxford (1999)
2. Reiss, A.G., et al.: Observational evidence from Supernovae for an accelerating universe and a cosmological constant. Astron. J. **116**, 1009–1038 (1998)
3. Garnavich, P.M., et al.: Supernova limits on the cosmic equation of state. Astrophys. J. **509**, 74–79 (1998)
4. Perlmutter, S.J., et al.: Discovery of a supernova explosion at half the age of the universe and its cosmological implications. Nature (London) **391**, 51–54 (1998)
5. Stuchlík, Z., Hledík, S.: Some properties of the Schwarzschild-de Sitter and Schwarzschild-anti de Sitter spacetimes. Phys Rev. D **60**, 044006 (1999)
6. Evans, J., Rosenquist, M.: $F = ma$ optics. Am. J. Phys. **54**, 876–883 (1986)
7. Evans, J., Nandi, K.K., Islam, A.: The optical-mechanical analogy in general relativity: exact Newtonian forms for the equations of motion of particles and photons. Gen. Relativ. Gravit. **28**, 413–439 (1996)
8. Nandi, K.K., Islam, A.: On the optical-mechanical analogy in general relativity. Am. J. Phys. **63**, 251–256 (1995)
9. Nandi, K.K., Migranov, N.G., Evans, J., Amedeker, M.K.: Planetary and light motions from Newtonian theory. An amusing exercise. Eur. J. Phys. **27**, 429–435 (2005)
10. Alsing, P.M.: The optical-mechanical analogy for stationary metrics in general relativity. Am. J. Phys. **66**, 779–790 (1998)
11. Hau, L.V., Harris, S.E., Dutton, Z., Behroozi, C.H.: Light speed reduction to 17 metres per second in an ultracold atomic gas. Nature (London) **397**, 594–598 (1999)
12. Nandi, K.K., Zhang, Y.Z., Alsing, P.M., Evans, J., Bhadra, A.: Analogue of the Fizeau effect in an effective optical medium. Phys. Rev. D **67**, 025002 (2003)
13. Leonhardt, U., Piwnicki, P.: Optics of nonuniformly moving media. Phys. Rev. A **60**, 4301–4312 (1999)
14. Leonhardt, U., Piwnicki, P.: Relativistic effects of light in moving media with extremely low group velocity. Phys. Rev. Lett. **84**, 822–825 (2000)
15. Visser, M.: Comments on "Relativistic effects of light in moving media with extremely low group velocity". Phys. Rev. Lett. **85**, 5252 (2000)
16. Marklund, M., Anderson, D., Cattani, F., Lisak, M., Lundgren, L.: Fermat's principle and variational analysis of an optical model for light propagation exhibiting a critical radius. Am. J. Phys. **70**, 680–683 (2002)

17. Ellis, H.G.: Ether flow through a drainhole: A particle model in general relativity. J. Math. Phys. **14**, 104–108 (1973)
18. Ellis, H.G.: Errata. J. Math. Phys. **15**, 520 (1974)
19. Nandi, K.K., Islam, A., Evans, J.: Brans wormholes. Phys. Rev. D **55**, 2497–500 (1997)
20. Nandi, K.K., Bhattacharjee, B., Alam, S.M.K., Evans, J.: Brans-Dicke wormholes in the Jordan and Einstein frames. Phys. Rev. D **57**, 823–828 (1998)